An 8-DPSK TCM Modem for MSAT-X

THOMAS C. JEDREY, NORMAN E. LAY, DR. WILLIAM RAFFERTY, Mobile Satellite Program, Jet Propulsion Laboratory, California Institute of Technology, United States.

Jet Propulsion Laboratory
4800 Oak Grove Drive
Pasadena, California 91109
United States

ABSTRACT

This paper describes the real-time digital implementation of an 8-DPSK trellis coded modulation (TCM) modem for operation on an L-band, 5 kHz wide, land mobile satellite (LMS) channel. The modem architecture as well as some of the signal processing techniques employed in the modem to combat the LMS channel impairments are described, and the modem performance over the fading channel is presented.

INTRODUCTION

Satellite based, mobile communications have received increasing attention over the past decade. NASA, through the Jet Propulsion Laboratory, initiated a land mobile satellite experiment (MSAT-X) program [1] with the explicit goal of developing enabling concepts and technologies for a mobile satellite service. Of the many issues addressed in the program, modulation and coding were recognized as a key system consideration given the available spectrum and the satellite power limitations, and the hostile nature of the transmission channel.

Early in the program, frequency division multiplexing was selected as the preferred channel structure to maximize the number of users. The channel bandwidth was set at 5 kHz for a data transmission rate of 4800 bits per second (bps). This was considered a formidable goal especially given the required bit error rate (BER) performance of .001 at an average bit signal to noise ratio (SNR) of 11 dB for the channel model described below. Analysis of the link requirements has led to the consideration and computer simulation of many coherent and non-coherent schemes for burst operation.

The L-band LMS channel is susceptible to many propagation impairments [2]. The traditional satellite model of a line-of-sight component in the presence of AWGN must be augmented to include dynamic effects. Multipath fading and vegetative shadowing cause signal dropouts and long term envelope amplitude and phase variations. The channel model assumed in the development of this modem is the Rician fading channel with a coherent (desired) to non-coherent (scattered) power ratio of 10 dB [2]. Vegetative shadowing is also assumed to be present and to follow a log-normal distribution.

The work described in this paper focuses on the digital implementation and performance of a multipath fade tolerant, differentially coherent, 8-PSK based modem. At the receiver, differential detection using a novel matched filter arrangement, and feed forward Doppler compensation is employed to achieve many operational benefits. For this demanding L-band satellite link, the channel utilization is an efficient 1.0 bps/Hz for raw data and 1.5 bps/Hz for coded data.

MODULATOR

A block diagram of the modulator is presented in Figure 1. The modulator obtains packetized data from the terminal processor at a rate of 4800 bps. A packet consists of a packet identification word, indicating a control or data packet, and the information to be transmitted, either voice or data. In addition to this structure, the modulator prefixes a preamble and appends a postamble to the transmitted packet, both of which are used for modem specific synchronization purposes, and are not encoded as described below.

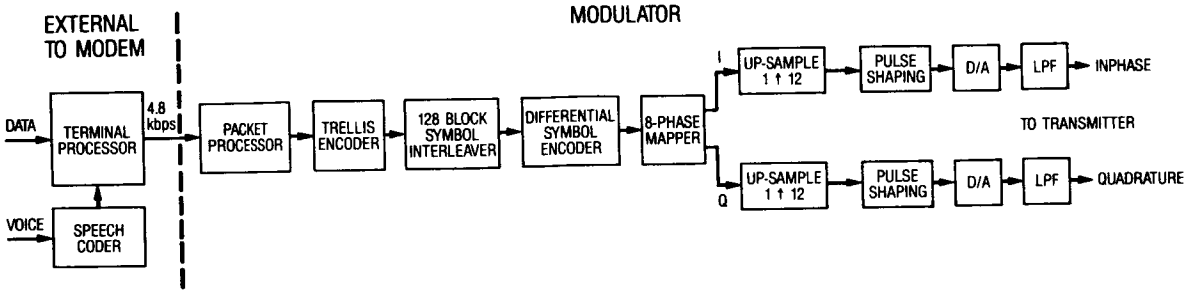

Figure 1 Modulator Block Diagram

The data to be transmitted is encoded with a rate 2/3, 16 state trellis code [3], producing a data rate of 7200 bps, or 2400 symbols per second. Following the encoder is a 128 symbol block interleaver (16x8) for burst error protection. The output of the interleaver is differentially encoded and converted to inphase (I) and quadrature (Q) components of an 8-DPSK waveform at the 2400 sample per second (sps) rate. This data is then upsampled to a rate of 28.8 ksps by zero padding and pulse shaped with a 100 percent excess bandwidth root raised cosine filter to achieve the desired spectral shape as well as satisfy certain temporal properties (two intersymbol interference (ISI) free points per symbol) necessary for Doppler estimation and matched filtering at the demodulator. The pulse shaping filters have an impulse response length equal to 6 symbol periods, with 12 samples per symbol. The resulting digital waveforms are converted to analog signals via two 12-bit D/A converters and lowpass filtered for image suppression. The baseband I and Q waveforms are then provided to the transmitter for complex modulation and transmission through the channel.

DEMODULATOR

A block diagram of the demodulator is presented in Figure 2. An important feature of the demodulator is the feed-forward nature of the processing as illustrated by the diagram. This type of architecture was chosen to combat the effects of the fading typical of the LMS channel. The architecture allows the demodulator to free wheel through deep fades and rapidly recover once the fade has ended (i.e., the signal level has returned to some nominal operational value).

The receiver presents the demodulator with the received signal at an IF frequency of 28.8 kHz. This signal is bandpass filtered for noise suppression and prechannel selection, and then sampled at four times the IF. Splitting the A/D output data into odd and even data streams, then decimating yields baseband I and Q data streams. Note that the resultant data streams are not time aligned (due to the use of a single A/D). To combat this potential source of degradation, prior to decimation the quadrature channel is interpolated to produce an estimate of the Q channel that is time aligned with the I channel. It can be shown that under ideal conditions, the interpolation reduces the relative error in the estimation of the received Q channel data at the ISI free points from approximately 4 percent to 0.1 percent.

The I and Q channels, at an aggregate data rate of 57.6 ksps are then lowpass filtered to the data bandwidth plus the maximum expected Doppler spread. These filters are implemented as 111 tap linear phase FIR filters. The samples out of the lowpass filters are then interpolated by a factor

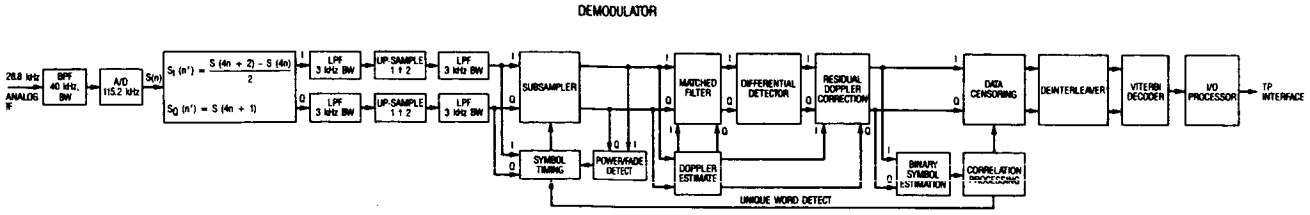

Figure 2 Demodulator Block Diagram

of two (the aggregate data rate is now 115.2 ksps) for reduction of jitter in the symbol timing recovery process, and passed on to the symbol timing and power/fade detect algorithms.

The power/fade detect algorithm corresponds to that of a modified radiometer. The I and Q channel data streams are squared and summed, lowpass filtered, and then thresholded. If the filter output exceeds the threshold, power is detected. If the filter output drops below a second threshold (once power and the start of a transmission have been detected) a fade is declared. The power/fade detect information is passed on with each symbol and used by the succeeding algorithms to reduce the effects of fades, as well as to reduce the preamble false alarm probabilities.

In the symbol timing algorithm, the received I and Q channel data is squared, summed, and bandpass filtered (centered at the symbol rate) to produce a sinusoidal timing wave of average period equal to the symbol rate [4]. This waveform is then clipped and differentiated to produce a sequence of impulses, corresponding to the zero crossings of the timing wave. The delay through the filtering is adjusted to align the positive impulses with the first ISI free symbol point per symbol period, and the negative impulses to the second. These timing impulses are used to sample the I and Q data streams at the ISI free points. It has been shown that the data dependent jitter in this timing algorithm is zero for the continuous case and approaches a constant dependent on the number of samples per symbol for the sampled data case, at these two points [5]. The impulses are also used to advance or retard a 4.8 kHz jitter clock, used to clock the Viterbi decoder output data to the terminal processor. The control mechanism for the jitter clock as well as the symbol timing algorithm is implemented as a random walk filter. In the free running or acquisition mode, the jitter clock can be advanced or retarded in steps of 1/24th of a symbol period per symbol period. In tracking mode, the jitter clock is only advanced (or retarded) after N net advances (or retards) have accumulated in an up/down counter. The acquisition mode corresponds to the preamble search (the preamble is designed to allow the symbol timing algorithm to quickly acquire correct timing) and the tracking mode corresponds to the detection of the preamble. Not only does this architecture provide a large measure of protection from fades and long runs of constant data, but it also utilizes the fade detect information to increase N during a long fade and to decrease N after the fade ends, thereby freezing the symbol timing during that period.

The subsampled data streams, sampled at the two ISI free points per symbol period are then passed on to a Doppler estimation, pseudo-matched filter, and differential detector. The Doppler estimator uses the two ISI free points per symbol period to strip the data from the received signal and derive an estimate of the Doppler [6]. This estimate is used to translate the pseudo-matched filter up to the Doppler frequency, where the matched filtering is done. This filter is termed a pseudo-matched filter due to the fact that only in combination with the ideal lowpass filters is it a true matched filter. In essence what has been implemented is a distributed form of the matched filter (primarily due to the fact that the matched filter for the 100 percent root raised cosine pulse shaping has a very simple realization). Following the matched filters, the data is differentially

detected and a residual Doppler term is removed. This architecture is described in [6] and illustrated in complex form in Figure 3. The aggregate data rate out of the residual Doppler correction is 4.8 ksps.

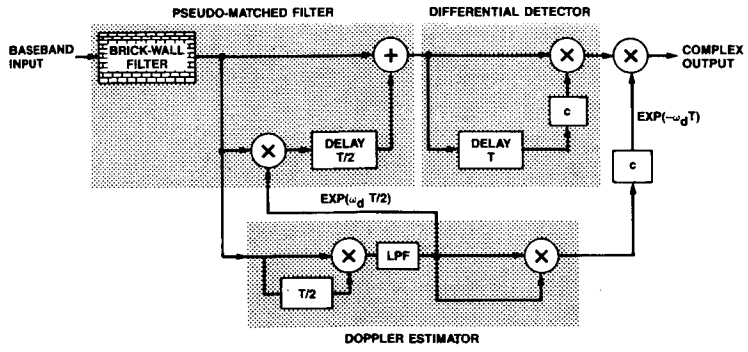

Figure 3 Complex Data Detection Block Diagram

Following the residual Doppler correction, the data is split into two paths, one for preamble/postamble detection, and the second for the actual data detection. The preamble/postamble detection algorithm is a correlator, with a detection declared in the case of the preamble if the threshold is exceeded and power is detected, and detection is declared in the case of the postamble if the threshold is exceeded within a certain time window (due to the fact that the postamble can only occur at fixed boundaries). The preamble and postamble are then censored from the received symbol stream.

The censored I and Q data streams, consisting of the received data symbols, are deinterleaved and decoded by a 16 state soft decision Viterbi decoder using the correlation metric. The decoder output is a 4800 bps data stream which is passed to the terminal processor. An indication of the data quality is also passed to the terminal processor by tagging the fade detect information to each bit as well as a 3-bit data quality estimate generated in the decoding process.

SYSTEM ARCHITECTURE

A completely programmable approach was chosen for the implementation of the digital signal processing elements of the MSAT-X modem. The flexibility afforded by a software based system allows both rapid realization and continual refinement for any variety of algorithms. In keeping with this approach, a general purpose signal processing board was developed utilizing a single DSP chip as the central element.

The core signal processor employed in the board is the Texas Instruments TMS32020. The signal processing board has a configuration of two 4K x 16 bit word spaces for program and data memory. In addition, the program memory is switchable between RAM for development purposes and EPROM for final algorithm placement. Additional circuitry supports five dedicated 16 bit parallel I/O ports (two input and three output). Three levels of hardware interrupt are accessible.

Within the modem itself, the modulator and demodulator are partitioned into two distinct systems under separate asynchronous control by an external controller. The multiprocessor design is greatly simplified by following a pipelined approach. Taken separately, the signal flow for either the modulator or demodulator can essentially be viewed as feed-forward for both control and data signals. This yields a very simple level of inter-board interfacing. Data is passed in parallel fashion sequentially from board to board on an interrupt basis. Signal processing algorithms are partitioned into a number of subprograms, each of which is executed on a single processor. The processing capability can therefore be incrementally increased by including more DSP boards and partitioning the new signal processing tasks into the additional processors.

The modulator consists of a single TMS32020 board, a clock unit (shared with the demodulator) and two D/A subsystems. The clock unit provides frequency locked clocks of 4.8 kHz and 28.8 kHz. The 4.8 kHz clock is used to transfer the data from the terminal processor to the modulator,

while the 28.8 kHz clock is used to transfer data from the TMS32020 board to the D/A subsystems. Each D/A subsystem consists of a 12 bit D/A converter and a 4 kHz lowpass filter.

The demodulator consists of an A/D subsystem, six TMS32020 boards, and two clock units. The A/D subsystem consists of a 40 kHz wide bandpass filter centered at 28.8 kHz, followed by a 12 bit A/D. The six TMS32020 boards are configured to implement the demodulator as illustrated in Figure 4. The first clock unit (common with the modulator) provides a clock at 18.432 MHz, which is divided down by the A/D subsystem to 115.2 kHz. The high clock rate allows slewing of the 115.2 kHz clock phase by the demodulator. The second clock unit is the 4.8 kHz jitter clock, used to transfer data from the demodulator to the terminal processor (this clock unit is also run from the 18.432 MHz clock unit). The clock phase of the jitter clock may be advanced/retarded by the demodulator to the data derived timing.

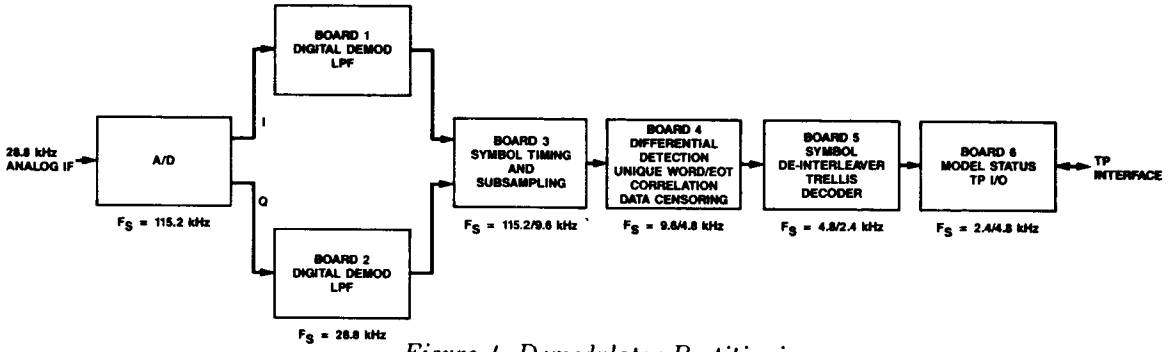

Figure 4 Demodulator Partitioning

MODEM PERFORMANCE

The modem has been tested over the land mobile satellite channel simulator described in [7]. The channel impairments simulated in these tests consist of AWGN and the Rician fading process. Symbol and bit error rates for the MSAT-X modem in the presence of AWGN are detailed in [8].

The modem performance in the presence of multipath fading with Rician K factors of 5 and 10 dB is shown in Figure 5. The signal-to-noise power calibration has a measurement error of approximately .2 dB due to the fluctuating signal level caused by the fading process. Two pairs of plots are shown in each figure comparing experimental performance to floating point simulation for Doppler spreads of 20 Hz and 104 Hz. These spread values correspond approximately to vehicle speeds of 8 mph and 44 mph at the L band link frequencies. As was expected, the modem performance is closer to the simulation results for the higher K value. However, for both values of K, the modem performs within 1 dB of the performance predicted by simulation. In these figures perfect doppler tracking and time synchronization are assumed for the simulation results.

CONCLUSIONS

The analysis of the experimental data has shown that the modem designed and constructed for MSAT-X will indeed function over the fading channel. In all cases for the conditions tested, the modem performs within 1 dB of theory/simulation. The architecture and processing algorithms in the modem allow the modem to combat the effects of deep fades and rapidly recover from them. Work is continuing on refining the modem, and in the near future a doppler estimation and correction scheme (this scheme has already been tested successfully with the demodulator in a slightly different configuration) will be implemented. Further tests will then be performed to determine its efficacy.

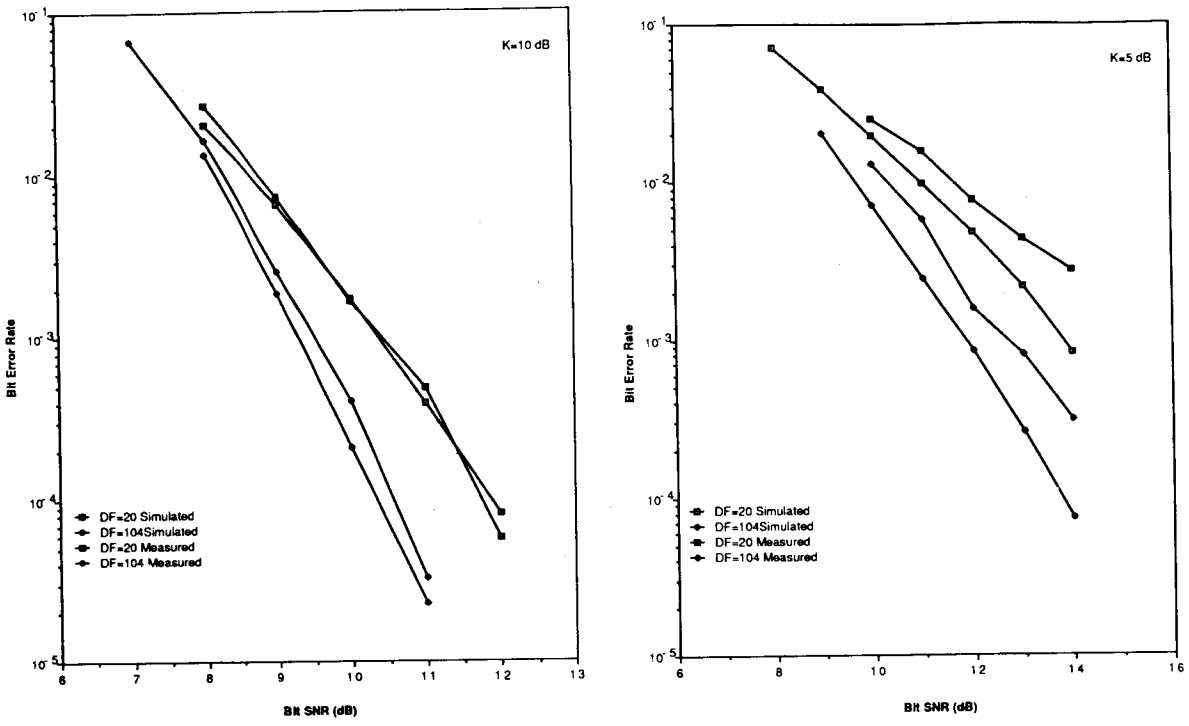

Figure 5 Trellis Coded 8-DPSK Performance in Fading Channel, K=10,5

REFERENCES

[1] E. J. Dutzi, G. H. Knouse, "Mobile Satellite Communication Technology: A Summary of NASA Activities', 37th Congress of the IAF, Innsbruck, Austria, October 1986.

[2] W. J. Vogel, E. K. Smith, "Theory and Measurements of Propagation for Satellite to Land Mobile Communication at UHF', Proc. IEEE 35th Vehicular Technology Conference, Boulder, Colorado, pp 218-223, 1985.

[3] D. Divsalar, M. K. Simon, "Trellis Coded Modulation for 4800-9600 bps Transmission over a Fading Mobile Satellite Channel", IEEE Journal on Selected Areas in Communications, February 1987, pp. 162-175.

[4] L. E. Franks, J. P. Bubrouski, "Statistical Properties of Timing Jitter in a PAM Timing Recovery Scheme", IEEE Trans. Comm., vol. COM-22, pp. 913-920, July 1974.

[5] T.C. Jedrey, unpublished memo.

[6] M. K. Simon, D. Divsalar, "Doppler-Corrected Differential Detection of MPSK", submitted to IEEE Transactions on Communications.

[7] F. Davarian, "Channel Simulation to Facilitate Mobile-Satellite Communications Research", IEEE Trans. Comm., vol. COM-35, pp. 47-56, 1987.

[8] T. C. Jedrey, N. E. Lay, W. Rafferty, "An All Digital 8-DPSK TCM Modem for Land Mobile Satellite Communications", IEEE International Conference on Acoustics, Speech, and Signal Processing, April 11-14, 1988, New York, New York.